An International Round-Robin Test for Insertion Impedance of Current Probes

Alexander Kriz[#1], Katsumi Fujii[2], David Knight[3], Dieter Schwarzbeck[4]

[1]Seibersdorf Laboratories, Austria

[2]National Institute of Information and Communications Technology, Japan

[3]National Physical Laboratory, United Kingdom

[4]Schwarzbeck Mess - Elektronik OHG, Germany

[#]alexander.kriz@seibersdorf-laboratories.at

***Abstract* — The insertion impedance of current probes could have a large influence on an EMC test result, but only limited information about this property is found in international standards and in scientific literature. An international round-robin test had been carried out to gain more experience about this property and its measurement. The proposed measurement method works well below 500 kHz but has problems above with capacitive coupling between probe and calibration fixture.**

***Keywords* — current probe, insertion impedance, transfer impedance, calibration fixture, EMC.**

I. Introduction

In CISPR 16-2-1 [1] methods for the measurement of disturbance currents on cables are described. Current probes (CPs) are used for this purpose, where specifications, construction examples and calibration methods are given in CISPR 16-1-2 [2].

Common mode currents on cables are crucial for the disturbance potential of electronic equipment. To measure them, current probes are clamped over conductors, where neither a conductive contact is made, nor the normal configuration is interrupted. The idea behind current probes is to build a transformer, where the conductor under test represents a one-turn primary winding and the secondary winding is contained within the current probe. The typical construction is a split cylindrical ferrite core, with a winding equally distributed on both sides of the core.

The voltage on the secondary side is proportional to the current through the conductor under test. This ratio is called transfer impedance and is determined by a calibration [2]. For the calibration the current probe is placed inside an expanded coaxial TEM system, called calibration fixture.

The current probe will cause a loading effect to the circuit. So, the current through the conductor under test is reduced. In an electric circuit model, an impedance called insertion impedance is introduced to account for this change.

II. Insertion Impedance

In CISPR 16-1-2 [2] the insertion impedance is specified to be less than 1 Ω for all current probes independent from its frequency range. Neither a definition for the insertion impedance nor a measurement procedure how to measure it is given. In CISPR 16-4-2 [3] the measurement uncertainty for conducted disturbance measurement is given. This standard uses the term insertion impedance also without giving further information.

Reference [4] describes the insertion impedance as the equivalent impedance, which appears to be in series with the circuit under test. Others [5,6,7] uses the term with the same meaning.

III. Probe Model

A schematic representation of a current probe is shown in Fig. 1. A formula for the insertion impedance is given by [5]

$$Z_{ins} = \frac{1}{N^2}\frac{R \cdot j\omega L}{R + j\omega L} - \frac{j\omega L}{\mu_r \cdot N^2} \quad (1)$$

With the secondary inductance L, the terminating resistor R, the relative permeability of the core μ_r and the turns ratio N.

Three different frequency sections can be seen in the frequency dependency. For low frequencies, where $R >> j\omega L$ and $\mu_r >> 1$, Eq. 1 is reduced to the first inductive term.

$$Z_{ins} = \frac{j\omega L}{N^2} \quad (2)$$

For medium frequencies where $R << j\omega L$ and $\mu_r >> 1$, the insertion impedance is resistive and frequency independent

$$Z_{ins} = \frac{R}{N^2} \quad (3)$$

With increasing frequency, the material parameter of the ferrite core will change. The relative permeability μ_r will decrease. For high frequencies, when μ_r is low, the insertion impedance is inductive, but with opposite phase

$$Z_{ins} = -\frac{j\omega L}{\mu_r \cdot N^2} \quad (4)$$

This principal behavior of the insertion impedance had been measured by [4,5,6].

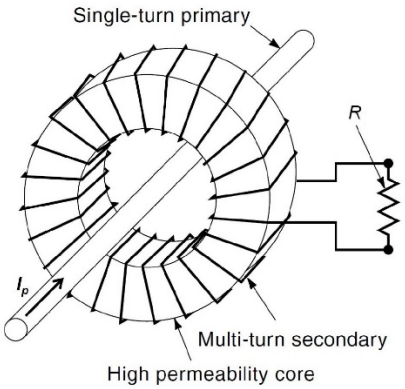

Fig. 1. Schematic representation of a current probe from [8]

IV. Measurement Method

Since the insertion impedance will increase the impedance of a circuit, the measurement principle will be to place the current probe in a suitable environment and to compare the impedance before and after the placement.

Calibration fixtures are used to calibrate the transfer impedance of current probes. They are widely spread in calibration laboratories. That is why they are chosen for the measurement method.

Since the expected insertion impedance is around 1 Ω a setup is required which will have enough sensitivity to measure this impedance correctly. The shunt-through method [9] is selected for this purpose, which is based on 2-port S-parameter measurement. The principle of this method is to connect both inner conductors of the test port cables and the unknown impedance to ground, see Fig.2. From the measured S_{21} the unknown impedance Z can be calculated.

$$Z = \frac{Z_0}{2}\frac{S_{21}}{1-S_{21}} \tag{5}$$

with the system impedance Z_0=50 Ω.

The measurement setup for insertion impedance measurement is shown in Fig. 3. Both port cables of the vector network analyser (VNA) are connected to one side of the calibration fixture via a T-connector, after a 12-term error correction had been performed.

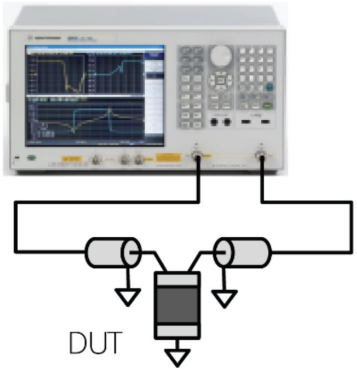

Fig. 2. Principle of shunt-through method from [9]

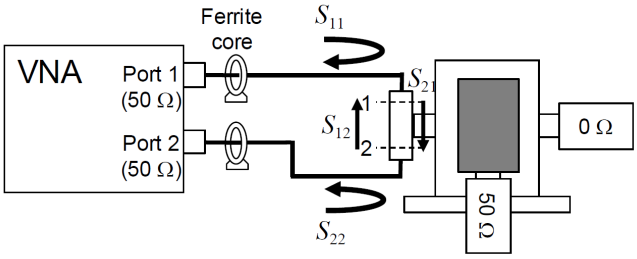

Fig. 3. Test setup for insertion impedance measurement

The second side of the calibration fixture is short circuited to keep the impedance of the circuit small. Ferrite cores are placed on the test cables of the VNA to avoid common mode currents.

The measurement is performed in two steps. First the impedance Z_1 of the empty calibration fixture is measured. After this, the current probe is inserted into the calibration fixture and the output of the probe is terminated with a 50 Ω load. The impedance Z_2 with the probe in place is measured.

The insertion impedance is calculated by subtracting both impedances

$$Z_{ins} = Z_2 - Z_1 \tag{6}$$

For the round-robin test only the absolute value of the impedance is taken into consideration. The phase is derived for information only.

V. Round-robin Test

A commercial current probe was chosen as test object. The frequency range is from 10 kHz to 100 MHz. The current probe was sent to four participating laboratories located in Austria, Germany, Japan and United Kingdom. Two of the laboratories carried out measurements in two different calibration fixtures. One of the laboratories delivered data only above 300 kHz due to limited resources. The total number of results is six.

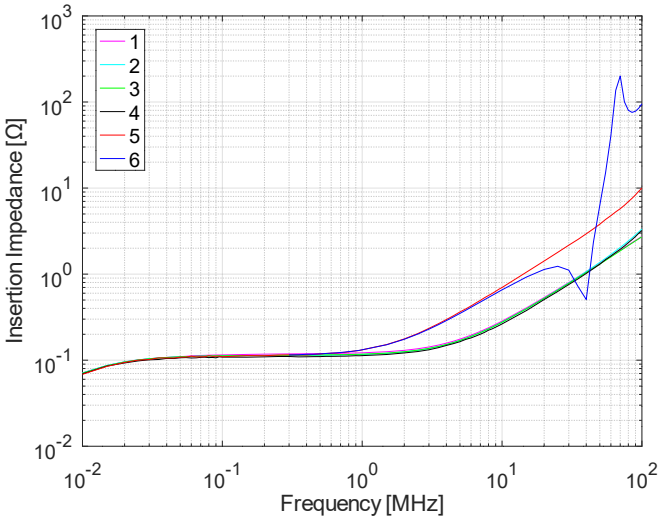

Fig. 4. Results of round-robin test

The anonymized results are shown in Fig. 4. The behaviour for absolute value and phase follows the probe model presented by [5] in chapter III. At 10 kHz the insertion impedance is around 70 mΩ, increasing to around 115 mΩ for the frequency independent section. The transition between those two sections is at 25 kHz.

Above 500 kHz the result splits into two groups. The first group, entitled group A, consists of 4 results and has a transition frequency to the high frequency section at 4 MHz and the insertion impedance rises to approx. 3 Ω. The second group, entitled group B, consists of two results with a transition frequency at 2 MHz. One of the results has a smooth response while the other one exhibits resonances.

VI. Analysis of Results

A. Frequency range below 500 kHz

For the frequencies below 500 kHz the results are stable, and a further analysis of the spread can be performed. Therefore, the average value, the minimum, the maximum and 95 % confidence interval (two times the standard deviation) for certain frequencies are shown in Table 1.

The spread of the results is low and the 95 % interval ranges from 3,3 % to 6,0 %. The measurement uncertainty can be estimated to be in the same range as the 95 % interval.

Table 1. Statistical analysis for results below 500 kHz

Frequency [kHz]	Average [mΩ]	Minimum/ Maximum [mΩ]	95 % interval [mΩ] / [%]
10	70,2	68,6 / 71,2	2,35 / 3,3
20	94,8	92,9 / 95,8	2,40 / 2,5
50	108,8	106,7 / 110,0	2,58 / 2,4
100	111,6	108,6 / 115,2	5,2 / 4,7
200	113,3	109,4 / 117,5	5,8 / 5,1
500	115,4	110,1 / 119,3	6,9 / 6,0

B. Frequency range above 500 kHz

All participants delivered information about the used equipment together with the test results.

One of the participants published two results (#4 and #5), one falling into each of the two groups. From comparison of the equipment list it was determined that the used calibration fixture was the only difference for both results. The two calibration fixtures are different in size and design, see Fig. 5. One of them is a closed design with rectangular side plates standing on an aluminium ground plane, see Fig. 5.a). The second one is an open design with no side and top plate, see Fig. 5.b). The length and height of the inner conduct is adjustable. The VSWR of calibration fixtures is nearly identical.

Comparing the designs of all used calibration fixtures revealed that group A consist of closed designs and group B of open designs.

The spread of results of group A is analysed. The average value, the minimum, the maximum and 95 % confidence interval for certain frequencies are shown in Table 2. The spread of the results is low below 100 MHz and the 95 % interval ranges from 4,5 % to 6,2 %. At 100 MHz it increased to 21,4 %.

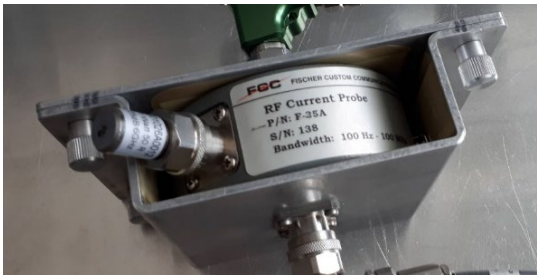

(a)

(b)

Fig. 5. Calibration fixture a) closed design b) open design

Table 2. Statistical analysis for group A above 500 kHz

Frequency [MHz]	Average [Ω]	Minimum/ Maximum [Ω]	95 % interval [mΩ] / [%]
1	0,117	0,113 / 0,122	7,2 / 6,2
5	0,170	0,164 / 0,176	9,5 / 5,6
10	0,275	0,264 / 0,284	16,8 / 6,1
50	1,330	1,304 / 1,370	60,5 / 4,5
100	3,004	2,718 / 3,347	642 / 21,4

VII. Calibration Fixture Influence

As shown in Chapter V the measured insertion impedance of a current probe depends on the used calibration fixture. Obviously, that cannot be correct since the insertion impedance is an intrinsic property of the current probe. A problem in the measurement method must be reason for this effect. To investigate the effect, the impedance Z_2 is analyzed for several test objects and compared to the impedance of the empty calibration fixture Z_1, see Fig. 6.

From the impedance Z_1, the inductance of the empty calibration fixture is calculated by $Z_1/(2\pi f)$ with approx. 60 nH.

The first test object is a commercial ferrite clamp on core. As expected, the ferrite core increases the impedance largely. The impedance is not a straight line in the log-log plot which indicates that the inductance reduces with frequency, due to the decrease of μ_r. The measured insertion impedance fits well to the values of the datasheet [10] given by the manufacturer.

After this measurement, a winding with 8 turns was placed on the core to simulate a current probe. The winding was short-circuited, which leads to a drastic reduction of the impedance compared to the ferrite core only. The phase of the insertion impedance is + 90° and the inductance is calculated by $Z_2/(2\pi f)$ – 60 nH with 19 nH. At 100 MHz the inductance increases to 25 nH, due to the decrease of μ_r.

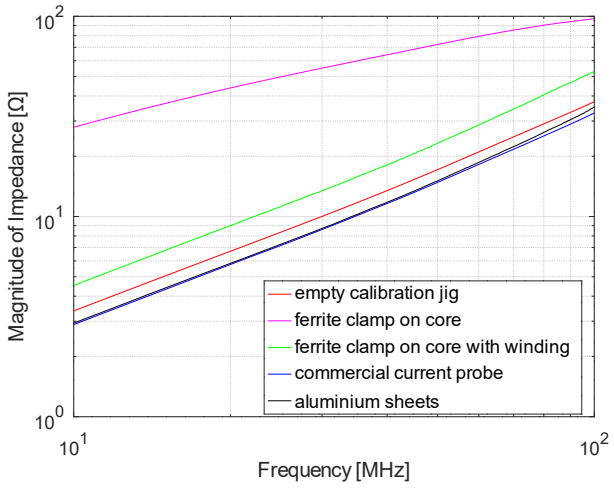

Fig. 6. Measured impedance of other test objects in calibration fixture

These results are in contradiction to the probe model given in chapter III. Setting R to zero in (1) will lead to

$$Z_{ins} = -\frac{j\omega L}{\mu_r \cdot N^2} \tag{7}$$

where the insertion impedance has the opposite phase angle.

Classical textbooks [11] give an equivalent circuit of a nonideal transformer including leakage fields, see Fig. 7. If resistive losses of the winding are neglected and a high coupling factor k is assumed, both leakage inductors can be combined. This will lead to an insertion impedance of

$$Z_{ins} = \frac{1}{{N_s}^2}\frac{R \cdot k \cdot j\omega L_p}{R + k \cdot j\omega L_p} + j\omega L_p 2(1-k) \tag{8}$$

For low and medium frequencies (8) is identical to (1), since $L=kL_p$ and $N_S=N$. In the high frequency range, the insertion impedance is dominated by the second term. This model fits to the recent observations.

Figure 6 also shows the impedance of the calibration fixture with a commercial current probe mounted (different model as used for the round-robin test). The commercial probe reduces the impedance to a value lower than the empty calibration fixture. This fits well to the assumption of a negative inductance in (7). The major difference between the commercial probe and the ferrite core with winding is the metallic housing of the commercial probe.

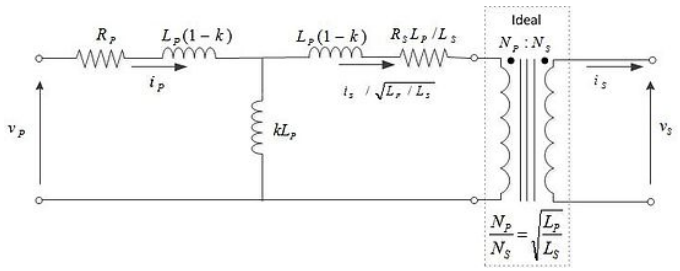

Fig. 7. Equivalent circuit of nonideal transformer from [12]

To simulate the effect of the housing two rectangular aluminum sheets (7 cm by 12 cm) are introduced to the calibration fixture. They are placed horizontally inside the calibration fixture, 2 cm above and below the inner conductor. The measured impedance (absolute value and phase) is nearly identical to the result of the commercial current probe. So, it is concluded that the rise of the insertion impedance in the upper frequency range is not a property of the current probe, but a capacitive coupling effect of the probe housing to the calibration fixture.

VIII. Conclusion

An international round-robin test was performed with four participants to investigate the measurement of the insertion impedance of current probes. The applied measurement method is easy to use and relies only on equipment that is already present in an EMC calibration laboratory.

Below 500 kHz the results fit together well with an estimated uncertainty of less than 6 %. Above 500 kHz large differences occur due to the influence of the used calibration fixture. Capacitive coupling between the current probe and the calibration fixture prevents reproducible measurements.

References

[1] *Specification for radio disturbance and immunity measuring apparatus and methods – Part 2-1: Methods of measurement of disturbances and immunity – Conducted disturbance measurements*, CISPR 16-2-1, Edition 3.0, ISBN 978-2-8322-1445-9, IEC, 2014-02

[2] *Specification for radio disturbance and immunity measuring apparatus and methods – Part 1-2: Radio disturbance and immunity measuring apparatus – Coupling devices for conducted disturbance measurements*, CISPR 16-1-2, Edition 2.1, ISBN 978-2-8322-5051-8, IEC, 2017-11

[3] *Specification for radio disturbance and immunity measuring apparatus and methods – Part 4-2: Uncertainties, statistics and limit modelling - Measurement instrumentation uncertainty,* CISPR 16-4-2, Edition 2.2, ISBN 978-2-8322-5950-4, IEC 2018-08

[4] L. M. Millanta, "Fundamentals of the EMC current probes", *Proc. 12th Int. Zurich Symp. Tech. Exhib.*, pp. 585-590, 1997-Feb.-1820.

[5] C. F. M. Carobbi and L. M. Millanta, "Circuit Loading in Radio-Frequency Current Measurements: The Insertion Impedance of the Transformer Probes," in *IEEE Transactions on Instrumentation and Measurement*, vol. 59, no. 1, pp. 200-204, Jan. 2010, doi: 10.1109/TIM.2009.2022450

[6] C. F. M. Carobbi and L. M. Millanta, "The Loading Effect of Radio-Frequency Current Probes," *2006 IEEE Instrumentation and Measurement Technology Conference Proceedings*, Sorrento, Italy, 2006, pp. 2050-2053, doi: 10.1109/IMTC.2006.328454.

[7] S. A. H. Razavi and S. Frei, "Characterization of current transformers for impedance measurements in automotive immunity test setups," *2016 International Symposium on Electromagnetic Compatibility - EMC EUROPE*, Wroclaw, Poland, 2016, pp. 411-416, doi: 10.1109/EMCEurope.2016.7739238.

[8] Xiao Hu, W. H. Siew, Martin D. Judd, Xiaosheng Peng, "Transfer function characterization for HFCTs used in partial discharge detection", IEEE Transactions on Dielectrics and Electrical Insulation, vol.24, no.2, pp.1088-1096, 2017

[9] Keysight, "Performing Impedance Analysis with the E5061B ENA Vector Network Analyzer", © *Keysight Technologies, 2017 – 2024, Published in USA, January 31, 2024, 5991-0231EN*

[10] *STAR-RING Snap Ferrite with safety key technology*, Würth Elektronik, Order. No. 7427155, www.we-online.com

[11] K. Küpfmüller and G. Kohn, „Theoretische Elektrotechnik und Elektronik," *15. Aufl. Springer-Verlag Berlin Heidelberg New York, 2000, ISBN 3-540-67794-1*

[12] „Leakage inductance", (2024) Wikipedia, available at: https:// https://en.wikipedia.org/wiki/Leakage_inductance (Accessed: 23.2.24)